Development 138, 3989-4000 (2011) doi:10.1242/dev.068866

The roles of maternal Vangl2 and aPKC in *Xenopus* oocyte and embryo patterning

Sang-Wook Cha, Emmanuel Tadjuidje, Christopher Wylie and Janet Heasman*

SUMMARY

The *Xenopus* oocyte contains components of both the planar cell polarity and apical-basal polarity pathways, but their roles are not known. Here, we examine the distribution, interactions and functions of the maternal planar cell polarity core protein Vangl2 and the apical-basal complex component aPKC. We show that Vangl2 is distributed in animally enriched islands in the subcortical cytoplasm in full-grown oocytes, where it interacts with a post-Golgi v-SNARE protein, VAMP1, and acetylated microtubules. We find that Vangl2 is required for the stability of VAMP1 as well as for the maintenance of the stable microtubule architecture of the oocyte. We show that Vangl2 interacts with atypical PKC, and that both the acetylated microtubule cytoskeleton and the Vangl2-VAMP1 distribution are dependent on the presence of aPKC. We also demonstrate that aPKC and Vangl2 are required for the cell membrane asymmetry that is established during oocyte maturation, and for the asymmetrical distribution of maternal transcripts for the germ layer and dorsal/ventral determinants VegT and Wnt11. This study demonstrates the interaction and interdependence of Vangl2, VAMP1, aPKC and the stable microtubule cytoskeleton in the oocyte, shows that maternal Vangl2 and aPKC are required for specific oocyte asymmetries and vertebrate embryonic patterning, and points to the usefulness of the oocyte as a model to study the polarity problem.

KEY WORDS: Vangl2, aPKC, Polarity, VAMP1, Oocyte, *Xenopus*

INTRODUCTION

The property of 'cell polarity' is fundamental to the differentiation, proliferation and morphogenesis of multicellular organisms, and abnormal cell polarity is a feature of cancer cells. Polarity influences embryonic development and tissue homeostasis in many ways, including the regulation and partitioning of cytoplasmic determinants, the positioning of organelles including nuclei, cilia, hairs and cell processes, the arrangement of the cytoskeleton and the regulation of both intracellular and extracellular trafficking of proteins.

Cell polarity can be defined in terms of both sheets of cells and the orientation of their organelles (e.g. cilia or wing hairs) with respect to the body axis (termed planar cell polarity, PCP) (for a review, see Vladar et al., 2009), and also in terms of an individual cell's polarity with regard to nuclear and cell process positions, or for epithelial cells, apical and basolateral surfaces, as defined by junctional structures and apical specializations such as brush borders (termed here apical basolateral polarity, ABP) (for a review, see Goldstein and Macara, 2007). Genetic and molecular analyses have indicated that both PCP and ABP systems are complex, consisting of several modules of interacting proteins, and that most of the components have been conserved throughout the metazoa. The PCP pathway in the *Drosophila* wing epidermis involves a global module, consisting of the atypical cadherins Fat and Dachsous and the Golgi-resident protein Four-jointed, that provides directional cues (Ma et al., 2003; Matakatsu and Blair, 2004; Simon, 2004; Strutt and Strutt, 2002; Yang et al., 2002), a core module, including the multi-pass transmembrane proteins Frizzled, Van Gogh (Strabismus) and Starry night (Flamingo) and the cytoplasmic proteins Dishevelled, Diego and Prickle, that aligns neighboring cells (Chae et al., 1999; Strutt, 2001; Tree et al., 2002; Usui et al., 1999; Vinson et al., 1989; Taylor et al., 1998; Wolff and Rubin, 1998), and a third group consisting of tissue-specific effector modules (Zeng et al., 2010; Heydeck et al., 2009; Gray et al., 2009). The ABP system consists of at least three modules. For example, in *Drosophila melanogaster* embryos, a reciprocal mutual exclusion system maintains the serine/threonine kinase atypical PKC (aPKC) and PDZ domain proteins Par-6 and Par-3 (Baz) asymmetrically localized in the apical membrane, and the serine/threonine kinase Par-1 in the lateral domain (for a review, see Macara, 2004), whereas in a second module the Crumbs protein (Crb) forms a complex with, and maintains the distribution of, Patj and Stardust (Sdt) at the apical/lateral boundary. The third module containing Lethal giant larvae [L(2)gL], Discs large (Dlg) and Scribble defines the basolateral domain, and is regulated by aPKC (Tian et al., 2008; for a review, see Mellman and Nelson, 2008).

Although in the above description the PCP and ABP pathways are considered separately, it is likely that they are interlinked. The tumor suppressor protein DLG1, generally considered to be part of one of the apical-basal polarity modules, has been shown to interact with Van Gogh protein in post-Golgi vesicles that are involved in plasma membrane formation in cellularizing *Drosophila* embryos (Lee et al., 2003), and the *Drosophila* ABP protein Scribble and the PCP protein Van Gogh have also been shown to interact (Courbard et al., 2009). Also, Prickle, which is normally considered to be a PCP core module component is important for the apical-basal polarity of epiblast cells in the mouse embryo, and interacts genetically with Vangl2 (the vertebrate homolog of Van Gogh) in this role (Tao et al., 2009). However, no link has been made between the functions of Vangl2 and aPKC.

Division of Developmental Biology, Cincinnati Children's Hospital Medical Center, 3333 Burnet Ave, Cincinnati, OH 45229, USA.

*Author for correspondence (heabq9@cchmc.org)

Accepted 4 July 2011

The ‘text-book’ description of ABP and PCP pathway components most easily fits sheets of epithelial cells, even though the proteins are also expressed in non-epithelial cells such as mesenchyme, muscle, neurons and oocytes, all of which display polarity. The full-grown *Xenopus* oocyte exhibits an animal-vegetal polarity with respect to its nuclear localization, and to the distribution of the cytoskeleton, yolk, pigment and some of its mRNAs and proteins. There is substantial evidence that the polarizations of cytoskeletal and membrane components as well as localized mRNAs and proteins in the oocyte provide information that determine body axes and zygotic gene expression in the developing embryo (reviewed in Marlow, 2010). In *Drosophila*, it has been shown that oocyte polarity depends on the ABP protein L(2)GL and its phosphorylation by aPKC, and LGL germline mutant clones showed disorganized microtubules and mislocalization of maternal determinants, including *staufen* and *oskar* mRNAs (Tian and Deng, 2008). However, the roles of vertebrate maternal Vangl2 and aPKC proteins in oocyte and embryo patterning are not understood.

Here, we describe the fact that Vangl2 is distributed in animally enriched islands in the subcortical cytoplasm in *Xenopus* oocytes where it interacts with a post-Golgi v-SNARE protein VAMP1. We show that Vangl2 is required for the stability of VAMP1 as well as for the maintenance of the stable microtubule architecture of the oocyte. We show that Vangl2 also interacts with aPKC, and that both the acetylated microtubule cytoskeleton and the Vangl2 and VAMP1 distribution are dependent on the presence of aPKC. We use antisense loss-of-function approaches to demonstrate that both aPKC and Vangl2 contribute to the patterning of the oocyte and early embryo by being required for the asymmetrical distribution of maternal transcripts for the germ layer and dorsal/ventral determinants VegT and Wnt11 and for apical-basal membrane polarity in the mature oocyte and early embryo. This study demonstrates the novel interaction and interdependence of the post-Golgi vesicle protein VAMP1, the PCP and ABP proteins Vangl2 and aPKC and the stable microtubule cytoskeleton in the oocyte and its importance for patterning the vertebrate embryo.

MATERIALS AND METHODS

Oocyte culture

For maternal mRNA and protein depletion, oocytes were injected with antisense oligonucleotides and cultured in oocyte culture medium (OCM) for 4 days (Mir et al., 2008). Although mRNA is depleted by oligonucleotide within 24 hours, it took 4 days for Vangl2 and aPKC proteins to be depleted to the levels shown in Fig. S2A in the supplementary material and Fig. 5C. The sequences (Table 1) and injection amounts (Table 2) of antisense oligonucleotides are shown in Tables 1 and 2. For cytoskeletal experiments, oocytes were incubated in OCM containing 5 μg/ml nocodazole (5 mg/ml stock in DMSO, Sigma) or 2 μM taxol (5 mM stock in DMSO, Sigma) for 2 hours and washed with fresh OCM before fixation. For GFP-LGL experiments, 1 mM progesterone was added to OCM (final concentration 2 μM in OCM) and the oocytes were cultured for 14 hours at 18°C for maturation. For the enzymatic removal of follicle cells (Fig. 5A), oocytes were washed with 1× MMR then incubated with 2 mg/ml of collagenase type 1 (Sigma) in 1× MMR for 30 minutes and the removal efficiency was checked with DAPI staining.

Histology

For general immunostaining, oocytes were fixed in ice-cold Dent’s fixative for 2 days at 4°C. For the acetylated tubulin staining, oocytes were fixed in ice-cold Dent’s fixative supplemented with 1 μM taxol for 1 day at 4°C to preserve the microtubule structure. Paraffin sections were obtained at 10 μm thickness. Section in situ hybridization samples were obtained by vibratome sectioning using a Leica VT1000S after embedding in a Fish gelatin/albumin mixture (Breckenridge et al., 2001).

Table 1. Sequences of antisense oligonucleotides and RT-PCR primers

Oligonucleotide names	Sequences (5′-3′)
VG AS4MP	T*G*G*CGCTGTCCTCCA*T*G*T
VG AS5MP	G*T*G*TCTAGAGCAGTC*C*A*G
Celsr1 AS3MP	T*G*G*CAATACAGTTCC*A*G*C
Celsr1 AS10MP	A*G*G*TAGGTTTGCTTC*A*T*A
aPKC AS5MP	C*T*A*GGTTGTCTTGGC*T*T*C
aPKC AS6MP	C*T*G*CTGTTCATTGCC*T*C*T
VG/Vangl2 U	GAGCGGCATCGATCTAAAAG
VG/Vangl2 D	GCAATAACAACCCCAAGGTG
Celsr1 U	GCAGCAACTCAGGATGTTCA
Celsr1 D	TTTATTCCACGCAGGGTCTC′
aPKC U	ACAGTGAACCAGAATTGCCC
aPKC D	CCGGACGAGCAGAACTTTAG

Asterisks represent phosphorothioate bonds between bases.
Sequences for ornithine decarboxylase (ODC), *Siamois*, *Xnr3* and *Foxi1e* primers were as previously published (Cha et al., 2008).

Western blot and immunostaining

Western blots were carried out as described (Cha et al., 2008). Antibody concentrations for western blot were: anti-PKC antibody (1:1000; C-20, Santa Cruz), anti-VAMP1 antibody (1:1000; Pierce) and anti-alpha tubulin (1:5000; DM1A, Neomarker). Immunostaining was performed with anti-Vangl2 antibody (1:200; M-13, Santa Cruz), anti-*Xenopus* Celsr1 antibody (1:250; custom antibody, Openbiosystems), anti-aPKC antibody (1:200; C-20, Santa Cruz), anti-acetylated tubulin (1:400; sc-23950, clone 6-11B-1, Santa Cruz), anti-VAMP1 antibody (1:200; Pierce) and anti-GFP(FL) antibody (1:200; sc-8334, Santa Cruz) followed by various fluorophore-conjugated secondary antibodies (Jackson Laboratory). Whole oocyte images were taken using a 10× objective on an Axioplan2 microscope and stitched using Adobe Photoshop software. Confocal images were taken with the Zeiss LSM510 system with LSM/ZEN software. For higher magnification images, oocytes were cleared with Murray’s clear and examined using a 63× C-Apochromat objective with digital zoom.

Co-immunoprecipitation assay

Oocytes were frozen in batches of 100 and lysed with 1 ml (10 μl/embryo) ice-cold PBS buffer containing 1% Triton X-100 with protease inhibitors. The homogenate was spun at 500 ***g*** for 5 minutes at 4°C; the supernatant was collected in a new tube and spun at 14,400 ***g*** for 10 minutes at 4°C. The clear lysate was mixed with protein-G agarose beads coated with the antibody of interest and incubated for 2 hours at 4°C. The beads were pelleted, washed four times with ice-cold lysis buffer, mixed with minimum volume of 4× SDS-PAGE sample buffer and processed through standard electrophoresis and western blot protocol using ice-cold CAPS buffer (0.2% CAPS, 15% MeOH, pH 10.5) for wet transfer and developed using an ECL Kit (Amersham).

Generation of mRNAs

For mRNA, *Xenopus laevis* Vangl2-V5 and *Xenopus tropicalis* GFP-LGL was linearized using *Not*I. All linearized constructs were transcribed by SP6 polymerase with mMessage mMachine Kit (Ambion).

Quantitative RT-PCR and in situ hybridization

Total RNA from oocytes, explants and early embryos was isolated using a previously published proteinase K-based protocol (Birsoy et al., 2006). Real-time RT-PCR was performed using a LightCycler (Roche). Water blank and RT-minus controls were included in all runs. All RT-PCR results are presented as percentages compared with the level in uninjected embryos or oocytes after normalization to the expression level of ornithine decarboxylase (ODC). Primer sets for *aPKC*, *Vangl2* and *Celsr1* are summarized in Table 1 and other primers for real-time PCR have been previously published (Cha et al., 2008). Whole-mount in situ hybridization was performed as described (Birsoy et al., 2006).

Table 2. Summary of the phenotypes caused by depletion of *Xstbm/Vangl2*, *XCelsr1* and *aPKC* mRNA from at least three experiments

	Phenotype [number observed (percentage of total)]		
Oligonucleotide name (amount injected)	Normal	Reduced head	Ventralized
Uninjected	83 (92.2)	6 (6.7)	1 (1.1)
VG AS4MP (6 ng)	2 (2.4)	61 (74.4)	19 (23.2)
VG AS5MP (6 ng)	5 (4.1)	81 (67.0)	35 (28.9)
Celsr1 AS3MP (7.5 ng)	2 (1.7)	101 (85.6)	15 (12.7)
Celsr1 AS10MP (10 ng)	9 (14.3)	45 (71.4)	9 (14.3)
aPKC AS5MP (5 ng)	1 (1.9)	14 (26.9)	37 (71.2)
aPKC AS6MP (10 ng)	0 (0.0)	32 (68.1)	15 (31.9)

Embryos and explants

The host transfer method was performed as described by Mir and Heasman (Mir and Heasman, 2008). Antisense oligonucleotides were injected on day 1 and oocytes were matured on day 3 and fertilized on day 4. The equatorial explants were obtained by removal of the animal caps and vegetal masses from late blastulae (Cha et al., 2008).

Luciferase assay

TOPflash DNA (50 pg; Upstate) together with 25 pg pRLTK DNA was injected into two dorsal vegetal cells at the 8-cell stage. Three replicate samples, each of three embryos, were frozen for each group at the late blastula stage and assayed using the Promega luciferase assay system.

RESULTS

Vangl2 interacts with the post-Golgi vesicle protein VAMP1 in *Xenopus* oocytes

The roles of PCP and ABP pathway components have not been examined in vertebrate oocytes, although real-time RT-PCR analysis shows that their mRNAs (including *Vangl2*, *Celsr1*, *Disheveled*, *frizzled*, *prickle*, *PTK7*, *aPKC*, *scribble*, *Par3* and *Par6*) are expressed (data not shown). In these experiments we focused first on the *Xenopus* homolog of *Drosophila* Van Gogh, Vangl2, because it plays pivotal roles in invertebrate and vertebrate planar polarized epithelia (reviewed in Vladar et al., 2009; Wansleeben and Meijlink, 2011), is expressed as a localized mRNA in *Xenopus* oocytes (see Fig. S2C in the supplementary material) and is the only PCP core component for which a mutation has been identified in human familial and sporadic cases of neural tube defects (Kibar et al., 2009; Kibar et al., 2011; Lei et al., 2011). We first examined the distribution of Vangl2 protein (Goto and Keller, 2002) in oocytes, by immunostaining with a Vangl2 specific antibody. Surprisingly Vangl2 was not located at the plasma membrane, but was found in radially arranged islands in the subcortical cytoplasm in both animal and vegetal hemispheres, with the animal hemisphere being particularly enriched (Fig. 1A,C,C′). The specificity of the staining was confirmed by depleting Vangl2 with a specific antisense oligonucleotide (see Fig. S1A,B in the supplementary material), which revealed loss of staining in these islands (Fig. 1E compared with 1D). When V5-tagged exogenous *Vangl2* mRNA was injected into oocytes, the overexpressed protein did not colocalize in these islands but accumulated at the cell membrane, suggesting that exogenous Vangl2 protein and endogenous Vangl2 protein were differently processed by the oocyte (Fig. 2A).

In contrast to the arrangement of endogenous Vangl2, the *Drosophila* Flamingo homolog Celsr1 (Morgan et al., 2003) was distributed throughout the cytoplasm, except in the radial islands containing Vangl2 (Fig. 1B,D,E). The custom-made Celsr1 antibody was also specific, because staining was lost as a result of depletion of Celsr1 using a specific antisense oligonucleotide (Fig. 1F; see Fig. S1B in the supplementary material).

To characterize further the Vangl2 islands, we compared their distribution pattern with that of the major cytoskeletal and membranous elements of the oocyte. The arrangement of stable microtubules revealed by an acetylated microtubule antibody partially overlapped to the pattern of Vangl2 staining (Fig. 2B), unlike that of cytokeratin filaments (see Fig. S2B in the supplementary material) or phalloidin stained actin filaments (Gard, 1999). Furthermore, depolymerization or stabilization of microtubules using nocodazole or taxol treatment caused the dispersal or co-redistribution of Vangl2 protein in both the animal and vegetal subcortical cytoplasm, suggesting an association of the Vangl2 islands with stable microtubules (Fig. 2C). Interestingly, the reverse was also true, i.e. Vangl2 was important for the maintenance of the acetylated microtubule array, as depletion of Vangl2 caused a reduction in the stable microtubule density in the subcortical regions of the oocyte (Fig. 2D).

As Vangl2 is a four-pass transmembrane protein we expected it to colocalize with a membranous component of the oocyte cytoplasm. The distribution of Vangl2 coincided with the staining of an antibody raised against the post-Golgi v-SNARE protein vesicle associated membrane protein 1, VAMP1 (synaptobrevin) (Aleu et al., 2002) (Fig. 3A for VAMP1), and not with markers for endoplasmic reticulum, Golgi, endosome, lysosome or retromer complex (data not shown). We confirmed that Vangl2 and VAMP1 colocalize by co-immunostaining (Fig. 3B) and that they interact physically by co-immunoprecipitation (Fig. 3C,D). Also, we found that overexpressed, exogenous Vangl2 decreased rather than increased the association of total Vangl2 with VAMP1, suggesting that it might act in a dominant-negative fashion.

To determine whether the interaction of Vangl2 with VAMP1 was restricted to a very specific role in oogenesis, we investigated whether Vangl2 and VAMP1 colocalized in tissues of the swimming tadpole. Vangl2 and VAMP1 vesicles were found to colocalize in specific sites in the embryo, in particular in epidermal epithelial cells, the smooth muscle of the gut and in single cells in the mesenchyme, consistent with a more general function for the interaction between these two proteins (Fig. 3E; data not shown).

Vangl2 regulates VAMP1 protein

The colocalization of Vangl2 and VAMP1 suggests either that Vangl2 is one of several proteins transported and/or stored in VAMP1 vesicles or that Vangl2 has a more structural interaction with VAMP1. To differentiate between these two possibilities, we investigated the effect of Vangl2 depletion on VAMP1 localization, by injecting an antisense oligonucleotide to *Vangl2* mRNA, and culturing the oocytes for 4 days before fixation. Confocal *z*-stack images of the animal area of control oocytes, collected as shown in Fig. 4A, showed the enrichment in this area with Vangl2 protein (Fig. 4B). Equivalent areas in sibling Vangl2-depleted oocytes

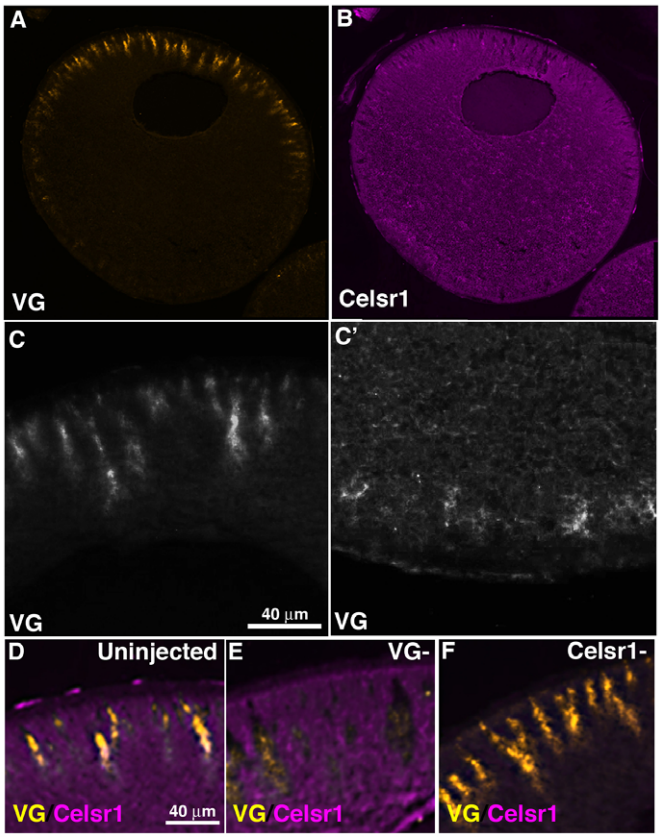

Fig. 1. Vangl2 and Celsr1 distribution in wild-type, full grown (stage 6) *Xenopus* oocytes. (**A**,**B**) Histological sections of stage 6 oocytes showing immunostaining pattern for Vangl2 (VG) protein (A) and Celsr1 protein (B). (**C**,**C′**), Higher magnification of animal (C) and vegetal (C′) hemisphere distribution of Vangl2 protein. (**D-F**), Images of animal hemisphere sections co-immunostained for Vangl2 and Celsr1 in uninjected control sibling (D), Vangl2-depleted (VG–; E) and Celsr1-depleted (Celsr1–; F) stage 6 oocytes.

showed a correlation between Vangl2 and VAMP1, such that areas lacking Vangl2 also lacked VAMP1 staining (Fig. 4C). The dependence of VAMP1 protein on the presence of Vangl2 was confirmed by western blotting, in which oocytes with reduced levels of Vangl2 also showed reduced amounts of VAMP1 protein (Fig. 4D). This suggests that Vangl2 is required for VAMP1 stability. This regulation was not dependent on the acetylated microtubule cytoskeleton as nocodazole treatment did not significantly reduce the amount of VAMP1 immunoprecipitated by Vangl2 (Fig. 4E), although taxol treatment, which dramatically increases the stable pool of microtubules, did increase the interaction (Fig. 4E). These data suggest that the architecture of the post-Golgi VAMP1 vesicles in the full-grown oocyte depends on an interaction with Vangl2 that is enhanced by, but not dependent on, polymerized microtubules.

Vangl2-VAMP1 distribution is dependent on aPKC

Because the distribution of Vangl2 and VAMP1 is dependent on the microtubule cytoskeleton, and in *Drosophila* oocytes the stable microtubule array is regulated by aPKC (Tian and Deng, 2008), we next aimed to determine whether the cytoskeleton and Vangl2-VAMP1 distribution were altered by aPKC depletion. Using an aPKC-specific antibody, we first showed that aPKC protein was distributed in the oocyte cytoplasm and at the animal and vegetal cell membranes and was present in both cytoplasmic and crude membrane fractions (Fig. 5A,B,D). We then determined that an antisense oligonucleotide directed against *aPKC* mRNA depleted the mRNA (see Fig. S1C in the supplementary material) and caused a reduction in aPKC protein levels (Fig. 5C). We then compared the acetylated microtubule cytoskeleton and arrangement of Vangl2 and VAMP1 proteins in control and aPKC-depleted oocytes after 4 days in culture. Figure 5E shows that depletion of aPKC had a dramatic effect on the oocyte acetylated microtubule cytoskeleton, causing its dispersal, although the total amount of alpha tubulin was unchanged (Fig. 5C). It also disrupted the Vangl2-VAMP1 islands, causing them to disperse and lose their subcortical radial arrangement (Fig. 5E′).

aPKC could affect Vangl2-VAMP1 localization directly or indirectly via its regulation of the stability of microtubules. We determined that aPKC interacts with Vangl2 by co-immunoprecipitation (Fig. 5G) and that this interaction was not susceptible to disruption by depolymerization of the microtubule cytoskeleton using nocodazole (Fig. 5G), suggesting that aPKC interaction with Vangl2 is not dependent on stable microtubules. Increased stabilization due to taxol treatment reduced the interaction of Vangl2 and aPKC, suggesting that it is dependent on non-polymerized tubulin (Fig. 5G). Also, VAMP1/Vangl2 interaction was not prevented by aPKC depletion (Fig. 5F), suggesting that VAMP1-Vangl2 vesicles were dispersed rather than broken down by aPKC depletion.

Embryonic patterning depends on both maternal Vangl2 and aPKC

It is well established that aPKC is essential in the asymmetrical localization of cell fate determinants in the *C. elegans* early embryo and *Drosophila* oocyte (Goldstein and Macara, 2007; Tian and Deng, 2008). However, the role of oocyte aPKC and Vangl2 protein in vertebrate oocyte and embryo asymmetries has not been established. Previous studies showed, and we confirmed, that aPKC protein is homogeneously distributed in *Xenopus* oocytes (Fig. 5A) until progesterone-induced maturation, when it becomes asymmetrically localized in the animal hemisphere (Nakaya et al., 2000). Next, we asked whether Vangl2 was required for this asymmetry. We showed for sibling oocytes that when control oocytes were matured, aPKC was cleared from the area at or near the cell membrane (Fig. 6A; 48/48 cases), whereas for Vangl2-depleted oocytes, aPKC remained in the vegetal area (Fig. 6A′; 41/45 cases), suggesting that Vangl2 is required for the redistribution of aPKC protein. The asymmetrical redistribution of aPKC in control oocytes was not due to degradation of vegetally localized protein because the total amount of protein did not change (data not shown).

Because, in epithelial cells, aPKC establishes apical versus basolateral domains by antagonizing the basolaterally localized LGL protein (Macara, 2004; Chalmers et al., 2003), we next examined the distribution of exogenous tagged LGL protein in *Xenopus* oocytes after *LGL-GFP* mRNA was injected. Figure 6B shows that in stage 6 oocytes LGL-GFP protein distributed at the cell membrane throughout the animal and vegetal hemispheres (Fig. 6B; 5/5). However, when oocytes were stimulated to mature by addition of progesterone to the medium, LGL-GFP protein concentrated in a patch at or near the plasma membrane in the vegetal hemisphere, and not in the animal hemisphere, in all cases examined (Fig. 6C; 16/16). This confirms that apical-basal polarity is established in the oocyte plasma membrane during maturation.

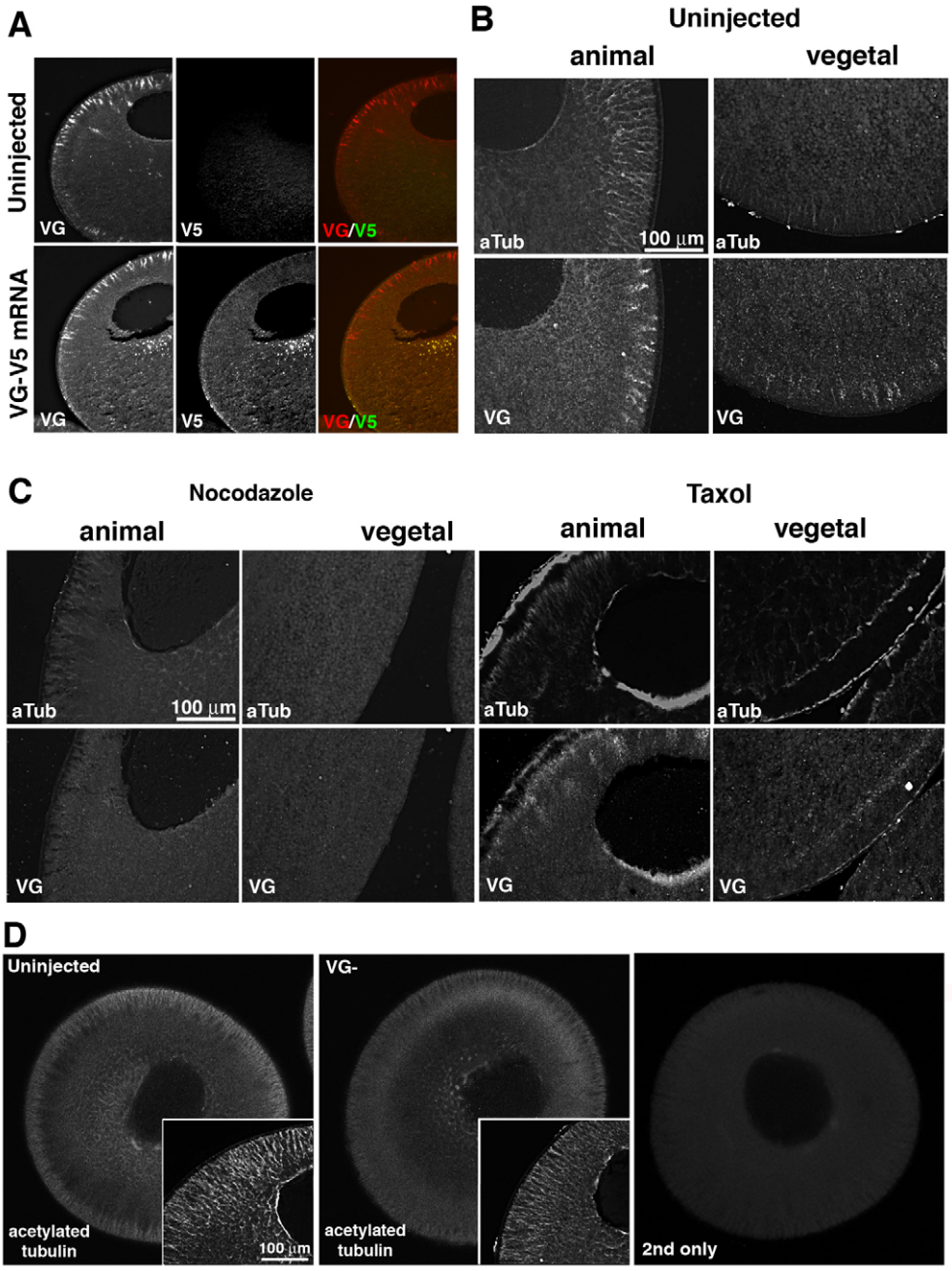

Fig. 2. Vangl2 protein distributes with and maintains the acetylated microtubule cytoskeleton. (**A**) Co-immunostaining of sections from uninjected and Vangl2-V5 mRNA (20 pg)-injected stage 6 *Xenopus* oocytes using Vangl2 (VG) and V5 tag (V5) antibodies. (**B**) Co-immunostaining of sections of wild-type stage 6 oocytes for acetylated tubulin (aTub) and Vangl2 (VG) in the animal and vegetal hemispheres. (**C**) Co-immunostaining for acetylated tubulin and Vangl2 protein in sections of nocodazole-treated (5 μg/ml) and taxol-treated (2 μM/ml) stage 6 oocytes. (**D**) Optical sections (2.6 μm thickness) of stage 6 control and Vangl2-depleted (VG–) oocytes stained as whole mounts to show the acetylated tubulin cytoskeleton. Insets show higher magnification images of histological sections stained with the same antibody. Right-hand panel shows a control whole mount stained with secondary antibody only.

By contrast, in histological sections of aPKC-depleted, mature oocytes stained for LGL-GFP (Fig. 6C; 12/12) and in Vangl2-depleted, whole-mount hemisected, mature oocytes stained for LGL-GFP (Fig. 6D; 6/7), LGL-GFP protein was not excluded from the animal hemisphere cell membrane. Thus, both Vangl2 and aPKC are required for these asymmetries of the oocyte plasma membrane that are established during maturation.

Next, we investigated whether maternal Vangl2 or aPKC were required for apical-basolateral membrane polarity in the early embryo by fertilizing Vangl2- and aPKC-depleted oocytes and analyzing the cell membrane distribution of overexpressed LGL-GFP protein. As shown in previous studies, LGL-GFP localized to basolateral membranes in blastula stage control sibling embryos (Fig. 6F). However, in both maternal Vangl2- and aPKC-depleted embryos, LGL-GFP was distributed on the apical membrane as well as basolaterally (Fig. 6F). This suggests that both maternal Vangl2 and aPKC are important in establishing apical versus basolateral membrane identity in the mature oocyte and the early embryo.

Next, because both Vangl2 and aPKC depletion affected the integrity of stable microtubules, which are known to be important for the localization of maternal determinants, we examined whether the depletion of either protein affected the distribution of known vegetally localized determinants: specifically, maternal *Wnt11* and *VegT* and *Xpat* mRNAs. In situ hybridization of control uninjected compared with Vangl2- and aPKC-depleted oocytes showed that depletion of either protein caused a loss of vegetally localized *Wnt11* and *VegT* mRNAs (Fig. 6G). By comparison, *Xpat* mRNA (Machado et al., 2005) was not affected by either Vangl2 or aPKC depletion (Fig. 6G). We showed by real-time RT-PCR that the

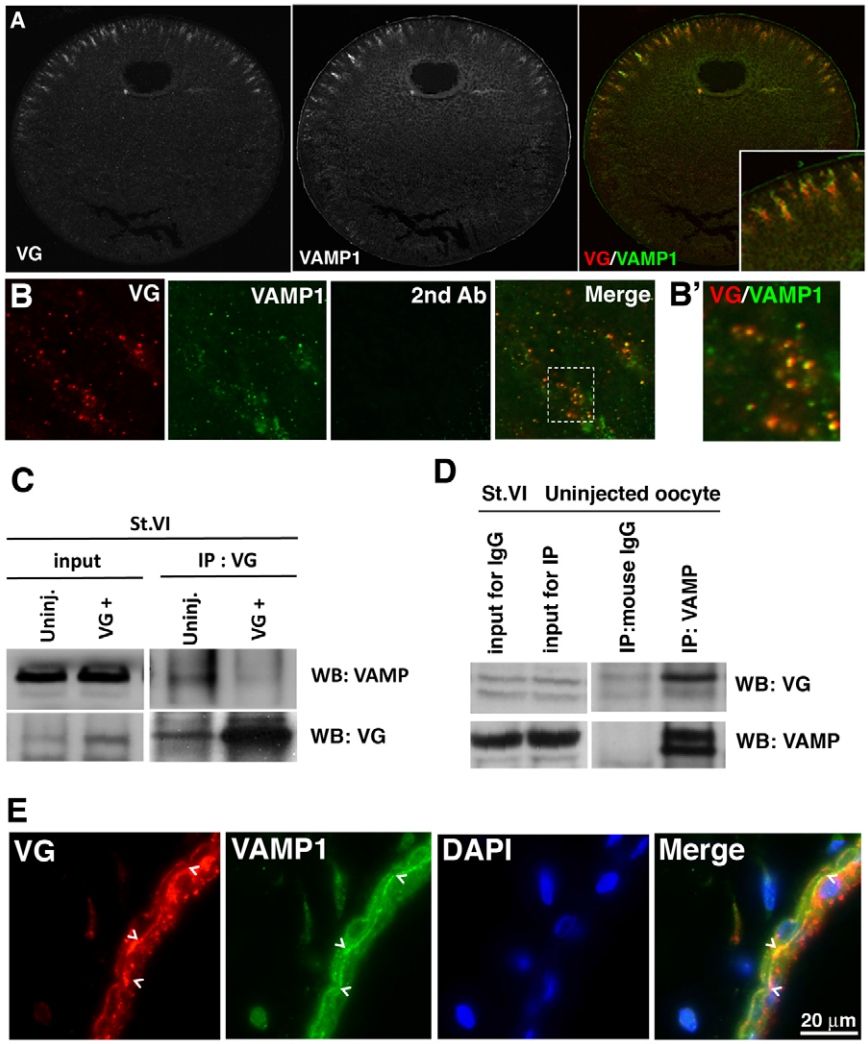

Fig. 3. Vangl2 interacts with VAMP1. (**A**) Histological section of a stage 6 *Xenopus* oocyte co-immunostained for Vangl2 (VG) and VAMP1. (**B**,**B′**) Colocalization of Vangl2 (red) and VAMP1 (green) in the stage 6 oocyte cytoplasm. B′ shows a high magnification image (×100 oil objective with digital zoom) of the boxed area in B demonstrating the co-distribution of Vangl2 and VAMP1 (yellow). (**C**) Co-immunoprecipitation analysis of lysates from wild-type and *Vangl2* mRNA (VG+; 500 pg)-injected stage 6 (St. VI) oocytes showing that endogenous Vangl2 protein (VG) interacts with endogenous VAMP1 protein (VAMP). Overexpressed Vangl2 reduces the total Vangl2 interaction with VAMP1. The expression level of VAMP1 in these samples is shown in the input lanes. (**D**) Co-immunoprecipitation analysis of an uninjected oocyte showing that endogenous VAMP1 protein interacts with endogenous Vangl2 protein. Mouse IgG serves as a negative control for non-specific binding of *Xenopus* oocyte lysates to the bead. (**E**) Co-immunostaining for Vangl2 (VG) and VAMP1 protein in histological sections of stage 45 tadpole skin. DAPI staining shows nuclei in the bilayered epidermis. Colocalization of VG and VAMP1 is most obvious on the basal side of the outer layer of the epithelium (chevrons, yellow staining in merge).

amounts of *VegT*, *Wnt11* and *Xpat* mRNA were unaffected by Vangl2 or aPKC depletion in sibling oocytes of those shown in Fig. 6G (Fig. 6H), suggesting that Vangl2 and aPKC depletion affected localization rather than stabilization of these mRNAs.

To examine whether disruption of the localized *VegT* and *Wnt11* mRNAs in the oocyte affected embryonic development, Vangl2- and aPKC-depleted oocytes were fertilized and allowed to develop to the early gastrula stage, at which time the regulation of zygotic gene expression by Wnt11 and VegT could be analyzed. Following both Vangl2 depletion and aPKC depletion, the embryos developed with reduced expression of the direct targets of the canonical Wnt signaling pathway *Xnr3* and *siamois* (Fig. 7A,C). The reduction in signaling in the canonical Wnt pathway was confirmed by TOPflash analysis (Fig. 7E). Also the endoderm marker *Xsox17*, which is a direct target of maternal VegT regulation and is normally expressed in the vegetal mass at the gastrula stage, was upregulated in the equatorial region of aPKC- and Vangl2-depleted embryos, whereas the mesodermal marker *Xbra* was unchanged (Fig. 7G,H). The ectopic expression of *Xsox17* was confirmed by in situ hybridization studies of control and Vangl2-depleted early gastrulae (Fig. 7G′). Furthermore, *Foxi1e*, a marker of embryonic ectoderm, was expressed in a 'salt and pepper' distribution in cells of the blastocoel roof in control embryos, but was upregulated and homogeneously expressed in all animal cells of the deep layer, and extended into the equatorial zone of aPKC- and Vangl2-depleted embryos (arrow in Fig. 7G,H). aPKC- and Vangl2-depleted tailbud-stage embryos showed phenotypes consistent with these early abnormalities, particularly failure of dorsal-ventral and anterior-posterior axis formation, the so called 'ventralized' phenotype (Fig. 7B,D,F). In the loss-of-function experiments carried out here, it was not possible to rescue the phenotypes of Vangl2-depleted embryos by injecting *Vangl2* mRNA, which might be due to the fact that protein synthesized from exogenous *Vangl2* mRNA trafficked to the cell membrane and did no colocalize with endogenous Vangl2 (Fig. 2A). By contrast, the aPKC-depleted phenotype was partially rescued by reintroduction of aPKC mRNA (data not shown). We confirmed that both the early gastrula and tailbud phenotypes caused by Vangl2 and aPKC depletion were specifically due to the loss of the respective proteins by repeating the experiments using a different antisense oligonucleotide against each mRNA (Fig. 7B,D). Thus, maternal aPKC and Vangl2 regulate the amount and position of expression of specific zygotic genes and are necessary for normal embryonic development.

DISCUSSION

Although genetic and biochemical studies have provided a great deal of information on the functions and interactions of Van Gogh/Vangl2 and aPKC, their activity is not understood. Here, we

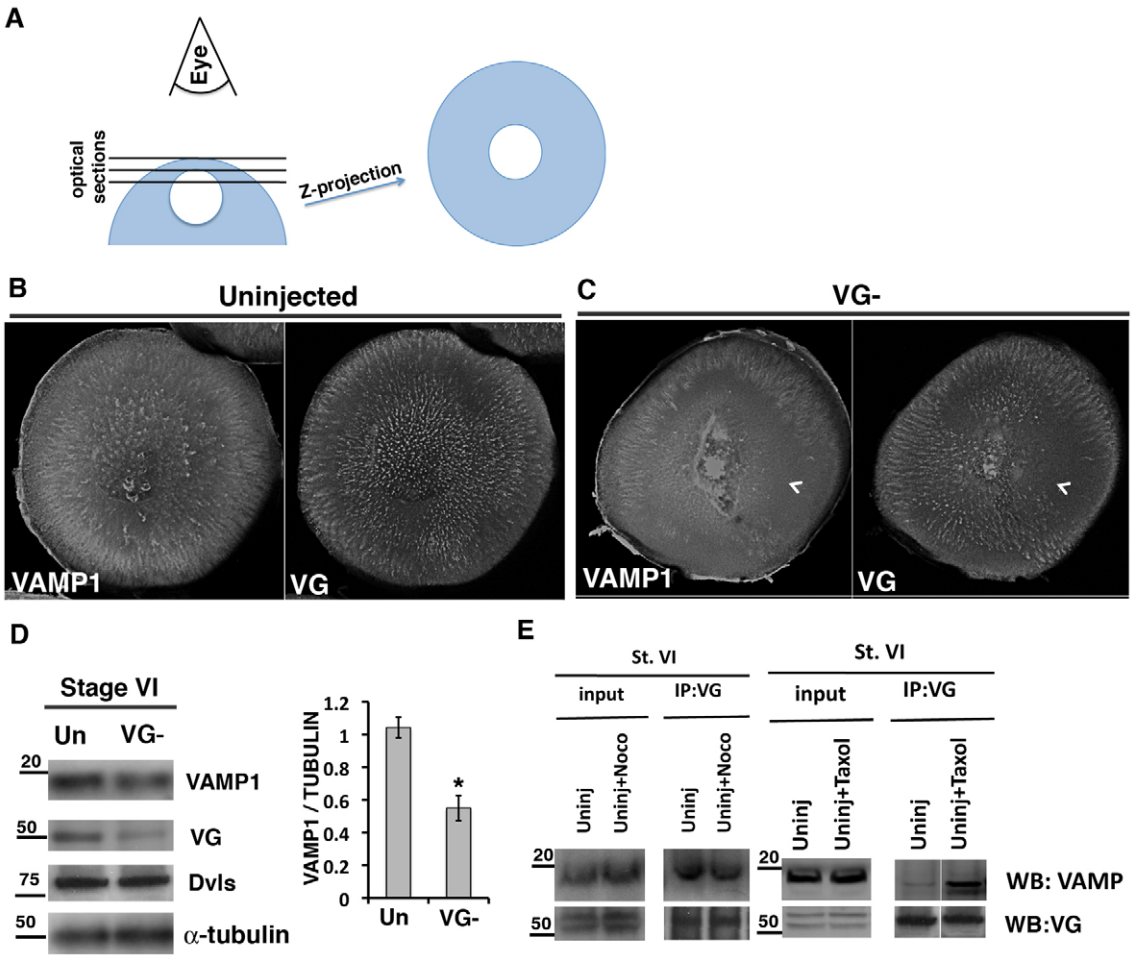

Fig. 4. Vangl2 is required for VAMP1 protein levels. (**A**) Diagram showing the procedure for generating the *z*-stack images shown in B and C. (**B**,**C**) *z*-stacks of the entire animal hemisphere projected as a single image for control (B, Uninjected) and Vangl2-depleted (C, VG–) stage 6 *Xenopus* oocytes, co-immunostained for VAMP1 and Vangl2 (VG) proteins. Chevrons point to areas that are devoid of both VAMP1 and Vangl2. (**D**) Western blot of lysates from stage 6 control (Un) and Vangl2-depleted (VG–) oocytes probed for VAMP1 and Vangl2. Antibodies against alpha-tubulin and *Xenopus* Disheveleds (Dvls) are used as loading controls. Quantification is shown for VAMP1 versus alpha tubulin for this experiment. The experiment was repeated with a similar result (*P<0.02, determined by *t*-test). Error bars represent s.d. (**E**) Co-immunoprecipitation analyses showing that endogenous Vangl2 protein interacts with VAMP1 in control (Uninj) and nocodazole (Noco)-treated stage 6 (St. VI) oocyte lysates, and that the interaction is increased by taxol treatment.

make several novel observations about their functions in the vertebrate oocyte. First, Vangl2 is localized in an animally enriched post-Golgi vesicle compartment, not as expected at the cell membrane, specifically interacting with the v-SNARE VAMP1. This is not an oocyte-specific phenomenon because VAMP1 and Vangl2 are also partially overlapping in the outer layer of the epidermis in the tadpole, as well as other tissues. In the epidermis, the non-colocalized Vangl2 is present in large aggregates, with unknown identity. We surmise that this might represent endocytosed protein or might be protein colocalizing with another VAMP family member. It is also noticeable in oocytes that, as shown both by immunostaining (Fig. 3A and Fig. 5B) and by co-immunoprecipitation (Fig. 3C,D), only a subset of Vangl2 protein interacts with VAMP1. Also, confocal images at higher magnification showed an asymmetry of this co-distribution, such that the most intense areas of colocalization are the areas nearest to the cell membrane (Fig. 5B). However, there was no evidence suggesting trafficking to the surface, because there was no obvious staining of either Vangl2 or VAMP1 at the plasma membrane itself (although VAMP1 is present in the single layer of follicular epithelium seen in Fig. 3A), and the areas of colocalization appeared to be at least 20-30 μm below the surface, beneath the pigmented cortex. Further understanding of this interaction requires immunostaining at the ultrastructural level.

We suggest that Vangl2 is not merely a cargo of this subset of vesicles but is involved in their maintenance, because loss of Vangl2 caused a loss of VAMP1 protein from the oocyte. In preliminary experiments examining changes in the amount of secretion into the medium of HA-tagged Wnt11 protein in control versus Vangl2-depleted oocytes [for collecting conditioned medium, a method described in Cha et al. (Cha et al., 2010) is used], we found (in three repeat experiments) that Vangl2 depletion increased the amount of Wnt11-HA secreted into the medium and reduced the amount of Wnt11-HA in the oocyte lysate, suggesting that Vangl2 might have a role in regulating the amount of secretion versus storage of secreted proteins. Much remains to be understood about the Vangl2-VAMP1 interaction, including its function in the oocyte, the nature of the vesicles' cargo and of other proteins

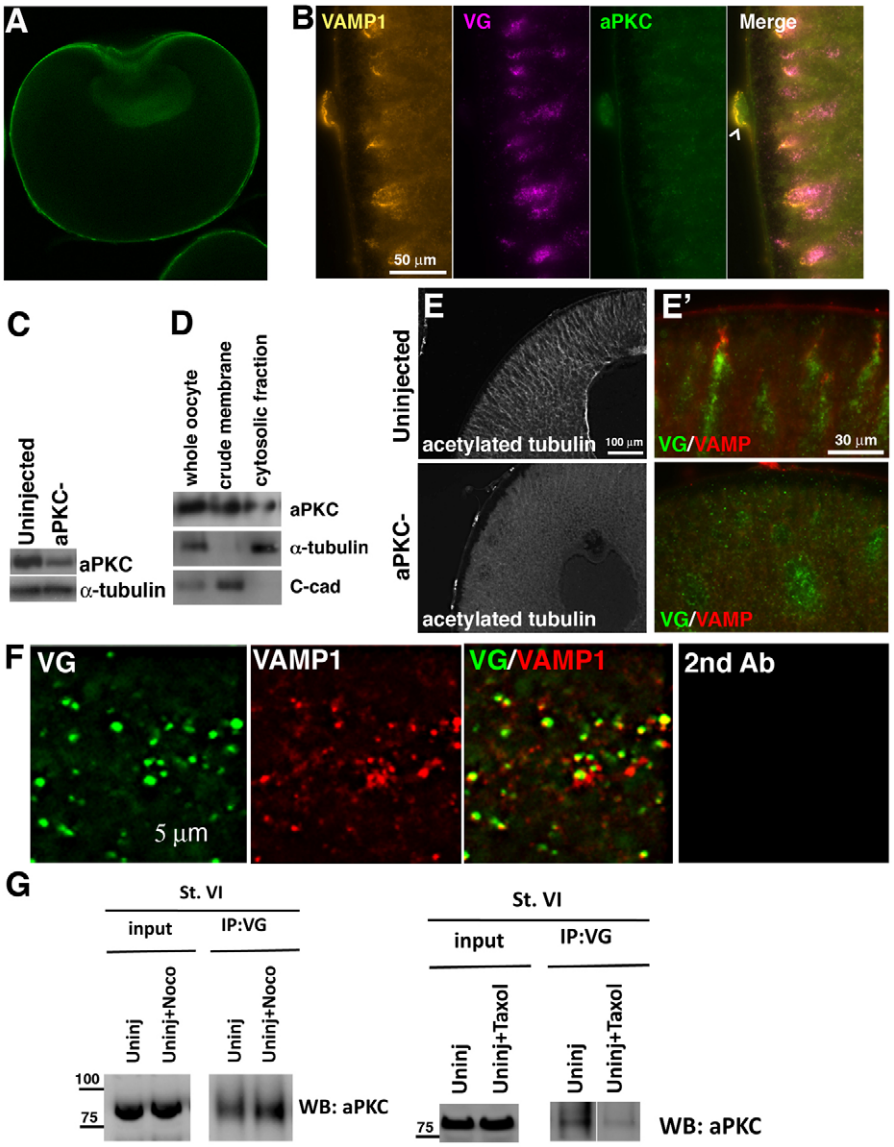

Fig. 5. aPKC regulates the distribution of the acetylated microtubule cytoskeleton and Vangl2-VAMP1 islands. (**A**) Histological section of a follicle-free (collagenase-treated) stage 6 *Xenopus* oocyte stained for aPKC protein. The nuclear staining is non-specific, as it is also observed in aPKC-depleted oocytes (not shown). (**B**) High magnification images of a histological section of the animal cortex of a control stage 6 oocyte co-immunostained for VAMP1, Vangl2 (VG) and aPKC. Chevron indicates a follicle cell. (**C**) Western blot showing aPKC protein levels in control and aPKC antisense oligonucleotide-injected (aPKC–) oocytes. (**D**) Western blot for aPKC using lysates from membrane and cytosolic fractions. Total α-tubulin is used as a marker for the cytosolic fraction and C-cadherin (C-cad) is used as a membrane fraction marker. (**E**,**E′**) Sections of control (upper panels) and aPKC-depleted (lower panels) stage 6 oocytes immunostained for acetylated tubulin (E) and Vangl2 (green) and VAMP1 (red) (E′). (**F**) Colocalization of Vangl2 (green) and VAMP1(red) proteins in aPKC-depleted oocyte cytoplasm. Right-hand panel shows incubation with secondary antibody only. (**G**) Co-immunoprecipitation analyses of lysates of control stage 6 (St. VI) oocytes showing that endogenous Vangl2 protein interacts with aPKC and that this interaction is not reduced by nocodazole (Noco) treatment (5 μg/ml) but is reduced by taxol treatment (2 μM/ml).

involved in the localization. Interestingly, other evidence also suggests a role for Van Gogh/Vangl2 in vesicle trafficking events. Van Gogh has been shown to recruit the tumor suppressor DLG to post-Golgi vesicles in TE85 cells, a function specific to Van Gogh as DLG did not have the reciprocal effect (Lee et al., 2003). In this case, the vesicles provided new plasma membrane for the cellularization of the embryonic blastoderm syncytium. It will be important to determine whether Vangl2 in the *Xenopus* oocyte has a similar role in the developing embryo, or whether it functions in other secretory roles in the oocyte. In the loss-of-function experiments described here the depletion of Vangl2 protein was incomplete and was clearly compatible with normal cleavage divisions. However, it is possible that further depletion of maternal Vangl2 protein with higher doses of oligonucleotide might prevent normal embryonic membrane formation.

It is interesting, and potentially important, to appreciate for overexpression experiments that Vangl2 protein derived from injected mRNA did not accumulate in the same sites as endogenous protein, and indeed caused a reduction of the interaction between VAMP1 and endogenous Vangl2, at least in the full-grown *Xenopus* oocyte. Further studies are needed to determine whether this is true in other planar polarity models, and also to analyze how overexpressed Vangl2 destabilizes the interaction of endogenous Vangl2 with VAMP1. Preliminary studies suggest that when the mRNA is injected into oocytes at an earlier stage of oogenesis (stage 3-4) there is colocalization of exogenous Vangl2 with VAMP1, suggesting that an element required for Vangl2 association with VAMP1 is present at stage 4 but not stage 6.

Second, we found that Vangl2 and aPKC depletion affected the cell membrane polarization of both matured oocytes and embryos at the blastula stage, as measured by the ability of overexpressed LGL protein to distribute in a polarized fashion. It has been shown previously that tagged LGL overexpressed in the animal cells of blastulae normally localizes to basolateral surfaces, as it does in many epithelia, and that this is disrupted by aPKC depletion (Chalmers et al., 2005). We confirmed this and showed that both maternal Vangl2 and aPKC are required to prevent LGL protein spreading to the apical membrane. We also confirmed the finding of Roberts et al. (Roberts et al., 1992) that the plasma membrane of full-grown oocyte does not have membrane polarity, and extend that observation to show that polarization of the membrane, at least with respect to the protein, occurs after progesterone-induced

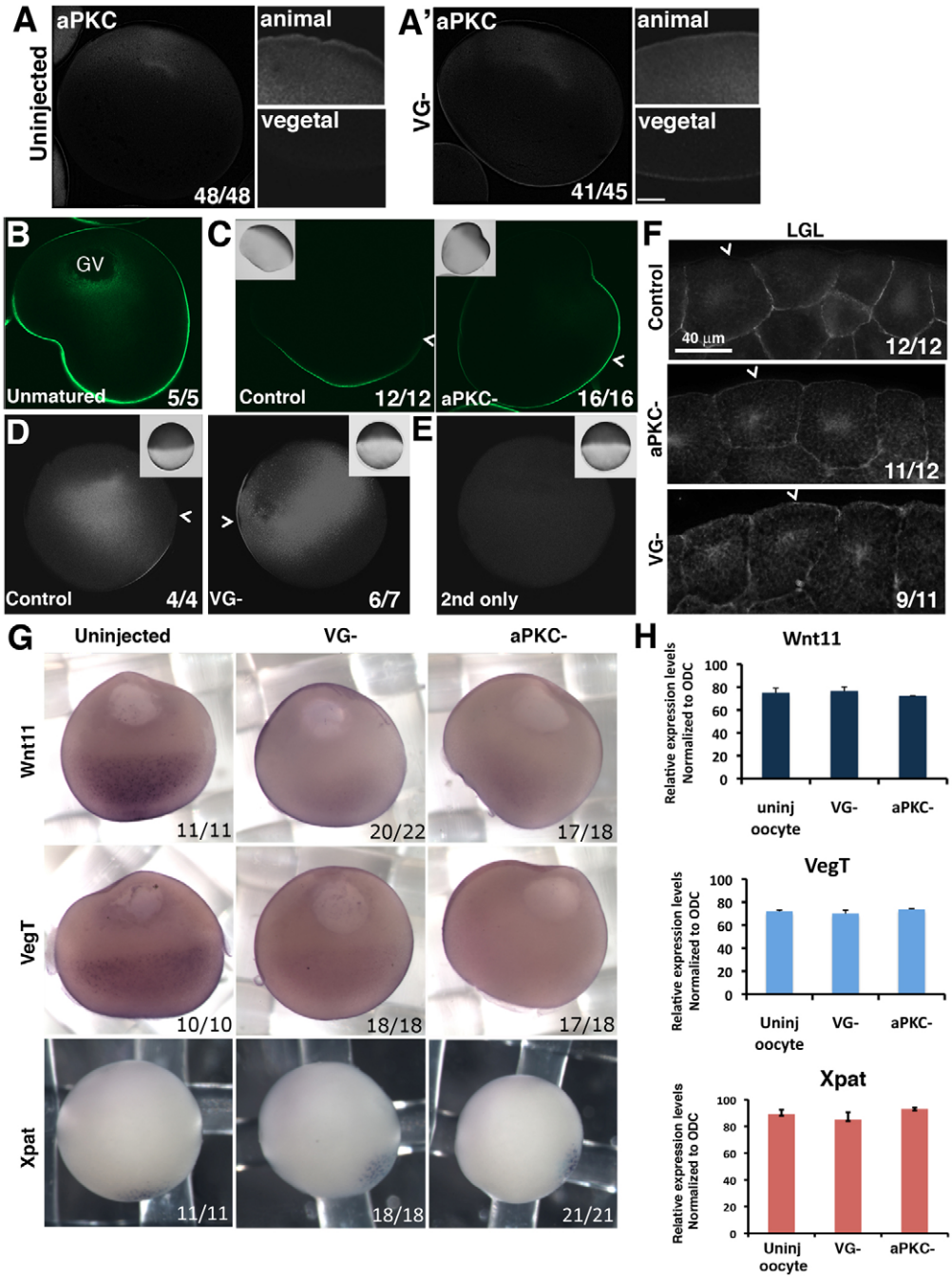

Fig. 6. Vangl2 and aPKC are required for specific oocyte membrane and mRNA asymmetries. (**A**,**A'**) Low and high magnification images of hemisected whole-mount, progesterone-matured control (A) and Vangl2 depleted (VG–; A') *Xenopus* oocytes stained for endogenous aPKC. (**B**,**C**) Localization of overexpressed GFP-LGL protein in anti-GFP immunostained histological sections of a stage 6 control oocyte (B) and progesterone-matured control and aPKC-depleted (PKC–) oocytes injected with *GFP-LGL* mRNA (C). Insets show bright-field images. Chevrons indicate the boundary between the animal and the vegetal hemispheres. (**D**) Comparison of the staining pattern of GFP-LGL in whole-mount anti-GFP immunostained control and Vangl2-depleted (VG–) progesterone-matured oocytes. Insets show the brightfield appearance of each oocyte and chevrons indicate the junction between animal and vegetal hemispheres. (**E**) Control for experiment shown in D showing a progesterone-matured oocyte that did not receive *GFP-LGL* mRNA injection. (**F**) GFP-LGL protein localization in histological sections of control, aPKC-depleted (aPKC–) and Vangl2-depleted (VG–) animal cells of embryos at the blastula stage, injected with *GFP-LGL* mRNA at the 2-cell stage. Chevrons mark the apical membrane of superficial cells in the animal cap. (**G**) In situ hybridization of sibling control, Vangl2-depleted (VG–) and aPKC-depleted (aPKC–) stage 6 oocytes probed for *Wnt11*, *VegT* and *Xpat* mRNAs. (**H**) Relative expression levels of *Wnt11*, *VegT* and *Xpat* mRNAs in control (uninj oocyte), Vangl2-depleted (VG–) and aPKC-depleted (aPKC–) oocytes determined by real-time RT-PCR (mean±s.d.).

maturation, because exogenous LGL protein is confined specifically to the vegetal cell membrane of the oocyte at this time and this localization is dependent on both Vangl2 and aPKC.

The third novel finding was that Vangl2 and aPKC loss of function resulted in a reduction in the acetylated microtubule cytoskeleton and loss of the localized *VegT* and *Wnt11* mRNAs. We have no evidence whether the role of Vangl2 in regulating the distribution of these mRNAs is linked to its association with VAMP1 vesicles. Also, we provide no direct evidence that the loss of the localized *VegT* and *Wnt11* mRNAs is due to the breakdown of the cytoskeleton, although previous studies suggest that this is likely to be the case. In *Drosophila* oocytes, oriented microtubules are necessary for the positioning of the polarized determinants *oskar*, *gurken* and *bicoid* mRNAs (Neuman-Silberberg and Schupbach, 1993; Nilson and Schupbach, 1999; van Eeden and St Johnston, 1999). In *Xenopus* oocytes, *Vg1* mRNA is dependent on intact microtubules for its localization in the vegetal cortex (Yisraeli et al., 1990; Kloc and Etkin, 1994), and, unexpectedly, both *VegT* and *Xlsrts* mRNA are necessary for the organization of other vegetally localized mRNAs and the cytokeratin cytoskeleton (Kloc and Etkin, 1994; Heasman et al., 2001; Kloc et al., 2005; Kloc et al., 2007). It is clear that there is not one single mechanism of localization as it has previously been shown that *Otx1* and *nanos1* localization is unaffected by VegT depletion (Heasman et al., 2001), and here we found that the germplasm component *Xpat* mRNA was not disrupted by Vangl2 depletion.

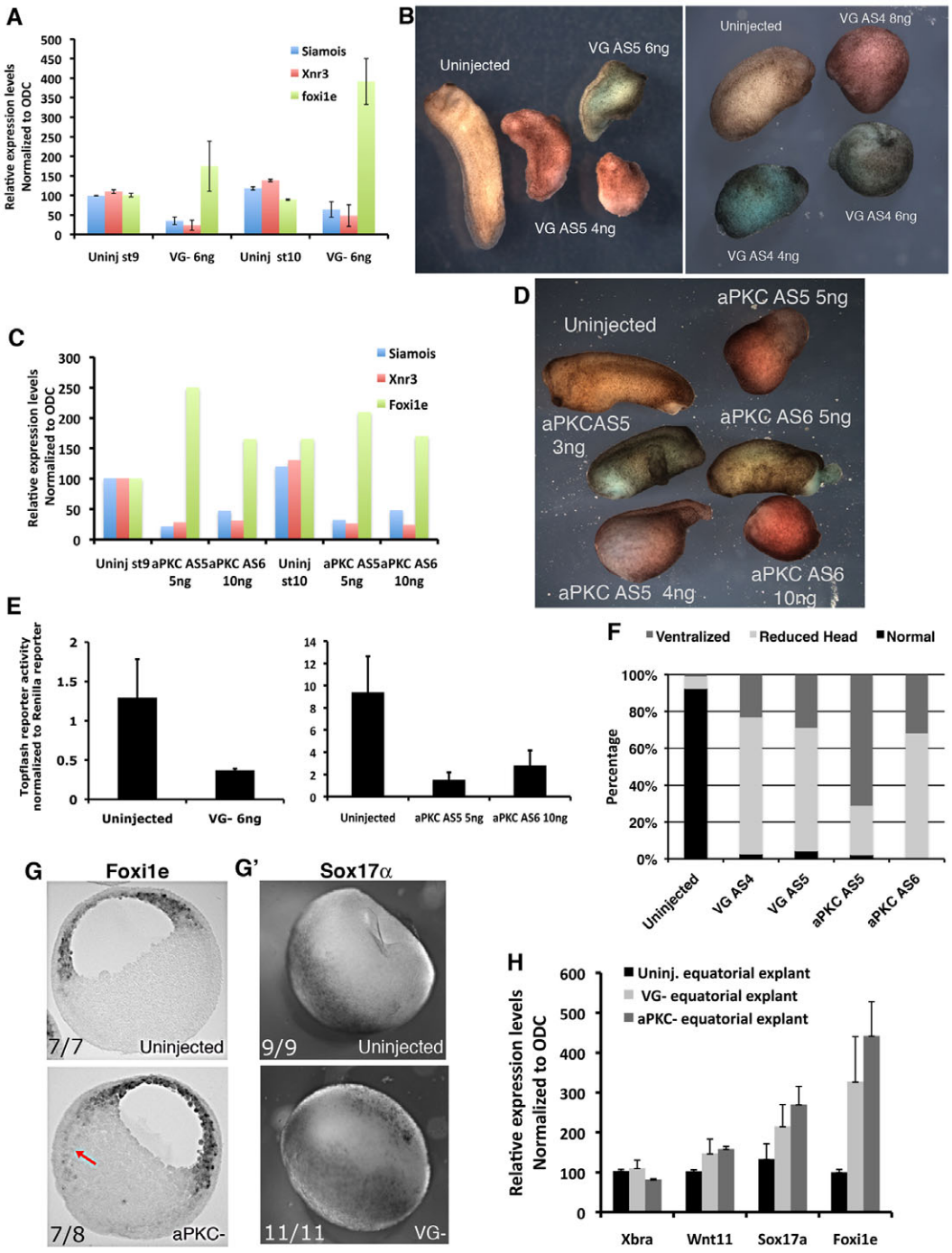

Fig. 7. Maternal Vangl2 and aPKC depletion disrupts the pattern of expression of specific zygotic genes. (**A**) Relative expression levels of *Siamois*, *Xnr3* and *Foxi1e* mRNAs in control (Uninj) and Vangl2-depleted (VG–) embryos at the late blastula (st9) and early gastrula stages (st10) determined by real-time RT-PCR (mean±s.d.). (**B**) Phenotype of embryos derived from sibling control (Uninjected) and Vangl2-depleted oocytes (VG AS5, 4 and 6 ng oligonucleotide injected; VG AS4, 4, 6 and 8 ng oligonucleotide injected) at the early tailbud stage. (**C**) Relative expression levels of *Siamois*, *Xnr3* and *Foxi1e* in control (Uninj) and aPKC-depleted embryos (AS5, 5 ng; AS6, 10 ng) determined by real-time RT-PCR at the late blastula and early gastrula stages. The experiment was repeated with a similar result. (**D**) Phenotype of embryos derived from sibling control (Uninjected) and aPKC-depleted oocytes (AS5, 3, 4 and 5 ng; AS6, 5 and 10 ng) at the early tailbud stage. (**E**) TOPflash reporter activation after injection into two dorsal vegetal cells of 8-cell stage control embryos compared with sibling Vangl2-depleted (left-hand graph) and aPKC-depleted (right-hand graph) embryos frozen at the late blastula stage, showing the reduction in canonical Wnt signaling activity (mean±s.d.). (**F**) Percentage of embryos with different phenotypes derived from Vangl2-depleted (AS4 and AS5), aPKC-depleted (AS5 and AS6) and sibling control at the tailbud stage. (**G**) Histological section of whole-mount stained, in situ hybridization of sibling control (upper) and aPKC-depleted (lower) early gastrulae using a *Foxi1e* probe. Arrow indicates ectopic expression of *Foxi1e* in the vegetal mass. (**G′**) Whole-mount in situ hybridization of sibling control (upper) and Vangl2-depleted (lower) early gastrulae using a *Sox17a* probe. (**H**) Relative expression levels of *Xbra*, *Wnt11*, *Sox17a* and *Foxi1e* in equatorial zones of control (Uninj.), Vangl2-depleted (VG–) and aPKC-depleted (aPKC–) embryos dissected at the late blastula stage and assayed by real-time RT-PCR (mean±s.d.).

Perhaps the most unexpected finding of this study was the fact that aPKC depletion and Vangl2 depletion caused similar phenotypes, and that those phenotypes included changes to zygotic gene expression in all three germ layers. In previous studies, overexpression of full-length *Vangl2/Xstbm* mRNA or *Vangl2/Xstbm* antisense 'morpholino' oligonucleotide injected into the 4-cell stage *Xenopus* embryo caused the classical 'convergence extension', open neural fold phenotype (Goto and Keller, 2002; Darken et al., 2002). Several considerations might explain the different phenotypes, convergence extension, caused by injecting a potentially dominant-negative form of Vangl2 after fertilization, and ventralization, caused here by depleting Vangl2 using an antisense oligonucleotide injected into the oocyte. First, we show here that overexpressed Vangl2 protein in the oocyte does not co-distribute with endogenous Vangl2, suggesting that exogenous overexpressed protein might not be processed in a similar fashion to endogenous protein or have the same binding partners and distribution as endogenous protein. In the loss-of-function experiments carried out here, it was not possible to rescue the phenotypes of Vangl2-depleted embryos by injecting *Vangl2* mRNA. Second, dominant-negative mRNAs injected after fertilization would be expressed too late to interrupt the oocyte functions of Vangl2, specifically the distribution of maternal determinants Wnt11 and VegT, and the membrane asymmetry that occurs during oocyte maturation.

In conclusion, although many questions remain to be answered, the data points to a link between the PCP and ABP pathways, suggesting that Vangl2 and aPKC are part of the same network of interactions that influence the cytoarchitecture of the egg via both the stable microtubule network and the vesicle trafficking system. This work suggests that the *Xenopus* oocyte provides an important new model to interrogate further the mechanisms of interaction of the PCP and ABP pathways and the roles of Vangl2 and aPKC proteins in particular.

Acknowledgements
We thank Amanda Shoemaker and Meredith McAdams for technical assistance, and Dr Ray Keller and Dr Nancy Papalopulu for supplying plasmids used in this study. This work was sponsored by NIH R01 GM084951. Deposited in PMC for release after 12 months.

Competing interests statement
The authors declare no competing financial interests.

Supplementary material
Supplementary material for this article is available at
http://dev.biologists.org/lookup/suppl/doi:10.1242/dev.068866/-/DC1

References
Aleu, J., Blasi, J., Solsona, C. and Marsal, J. (2002). Calcium-dependent acetylcholine release from Xenopus oocytes: simultaneous ionic currents and acetylcholine release recordings. *Eur. J. Neurosci.* **16**, 1442-1448.
Birsoy, B., Kofron, M., Schaible, K., Wylie, C., Heasman, J. (2006). Vg 1 is an essential signaling molecule in Xenopus development. *Development* **133**, 15-20.
Breckenridge, R. A., Mohun, T. J. and Amaya, E. (2001). A role for BMP signalling in heart looping morphogenesis in Xenopus. *Dev. Biol.* **232**, 191-203.
Cha, S. W. and Heasman, J. (2010). Using oocytes for Wnt signaling assays: paracrine assays and Wnt-conditioned medium. *Methods* **51**, 52-55.
Cha, S. W., Tadjuidje, E., Tao, Q., Wylie, C. and Heasman, J. (2008). Wnt5a and Wnt11 interact in a maternal Dkk1-regulated fashion to activate both canonical and non-canonical signaling in Xenopus axis formation. *Development* **135**, 3719-3729.
Chae, J., Kim, M. J., Goo, J. H., Collier, S., Gubb, D., Charlton, J., Adler, P. N. and Park, W. J. (1999). The Drosophila tissue polarity gene starry night encodes a member of the protocadherin family. *Development* **126**, 5421-5429.
Chalmers, A. D., Strauss, B. and Papalopulu, N. (2003). Oriented cell divisions asymmetrically segregate aPKC and generate cell fate diversity in the early Xenopus embryo. *Development* **130**, 2657-2668.
Chalmers, A. D., Pambos, M., Mason, J., Lang, S., Wylie, C. and Papalopulu, N. (2005). aPKC, Crumbs3 and Lgl2 control apicobasal polarity in early vertebrate development. *Development* **132**, 977-986.
Courbard, J. R., Djiane, A., Wu, J. and Mlodzik, M. (2009). The apical/basal-polarity determinant Scribble cooperates with the PCP core factor Stbm/Vang and functions as one of its effectors. *Dev. Biol.* **333**, 67-77.
Darken, R. S., Scola, A. M., Rakeman, A. S., Das, G., Mlodzik, M., Wilson, P. A. (2002).The planar polarity gene strabismus regulates convergent extension movements in Xenopus. *EMBO J.* **21**, 976-985.
Gard, D. L. (1999). Confocal microscopy and 3-D reconstruction of the cytoskeleton of Xenopus oocytes. *Microsc. Res. Tech.* **44**, 388-414.
Goldstein, B. and Macara, I. G. (2007). The PAR proteins: fundamental players in animal cell polarization. *Dev. Cell* **13**, 609-622.
Goto, T. and Keller, R. (2002). The planar cell polarity gene strabismus regulates convergence and extension and neural fold closure in Xenopus. *Dev. Biol.* **247**, 165-181.
Gray, R. S., Abitua, P. B., Wlodarczyk, B. J., Szabo-Rogers, H. L., Blanchard, O., Lee, I., Weiss, G. S., Liu, K. J., Marcotte, E. M., Wallingford, J. B. et al. (2009). The planar cell polarity effector Fuz is essential for targeted membrane trafficking, ciliogenesis and mouse embryonic development. *Nat. Cell Biol.* **11**, 1225-1232.
Heasman, J., Wessely, O., Langland, R., Craig, E. J. and Kessler, D. S. (2001). Vegetal localization of maternal mRNAs is disrupted by VegT depletion. *Dev. Biol.* **240**, 377-386.
Heydeck, W., Zeng, H. and Liu, A. (2009). Planar cell polarity effector gene Fuzzy regulates cilia formation and Hedgehog signal transduction in mouse. *Dev. Dyn.* **238**, 3035-3042.
Kibar, Z., Bosoi, C. M., Kooistra, M., Salem, S., Finnell, R. H., De Marco, P., Merello, E., Bassuk, A. G., Capra, V. and Gros, P. (2009). Novel mutations in VANGL1 in neural tube defects. *Hum. Mutat.* **30**, E706-E715.
Kibar, Z., Salem, S., Bosoi, C. M., Pauwels, E., De Marco, P., Merello, E., Bassuk, A. G., Capra, V. and Gros, P. (2011). Contribution of VANGL2 mutations to isolated neural tube defects. *Clin. Genet.* **80**, 76-82.
Kloc, M. and Etkin, L. D. (1994). Delocalization of Vg1 mRNA from the vegetal cortex in Xenopus oocytes after destruction of Xlsirt RNA. *Science* **265**, 1101-1103.
Kloc, M., Wilk, K., Vargas, D., Shirato, Y., Bilinski, S. and Etkin, L. D. (2005). Potential structural role of non-coding and coding RNAs in the organization of the cytoskeleton at the vegetal cortex of Xenopus oocytes. *Development* **132**, 3445-3457.
Kloc, M., Bilinski, S. and Dougherty, M. T. (2007). Organization of cytokeratin cytoskeleton and germ plasm in the vegetal cortex of Xenopus laevis oocytes depends on coding and non-coding RNAs: three-dimensional and ultrastructural analysis. *Exp. Cell Res.* **313**, 1639-1651.
Lee, O. K., Frese, K. K., James, J. S., Chadda, D., Chen, Z. H., Javier, R. T. and Cho, K. O. (2003). Discs-Large and Strabismus are functionally linked to plasma membrane formation. *Nat. Cell Biol.* **5**, 987-993.
Lei, Y. P., Zhang, T., Li, H., Wu, B. L., Jin, L. and Wang, H. Y. (2011). VANGL2 mutations in human cranial neural-tube defects. *N. Engl. J. Med.* **362**, 2232-2235.
Ma, D., Yang, C. H., McNeill, H., Simon, M. A. and Axelrod, J. D. (2003). Fidelity in planar cell polarity signalling. *Nature* **421**, 543-547.
Macara, I. G. (2004). Par proteins: partners in polarization. *Curr. Biol.* **14**, R160-R162.
Machado, R. J., Moore, W., Hames, R., Houliston, E., Chang, P., King, M. L. and Woodland, H. R. (2005). Xenopus Xpat protein is a major component of germ plasm and may function in its organisation and positioning. *Dev. Biol.* **287**, 289-300.
Marlow, F. L. (2010). *Maternal Control of Development in Vertebrates: My Mother Made Me Do It!*. San Rafael, CA: Morgan & Claypool Publishers.
Matakatsu, H. and Blair, S. S. (2004). Interactions between Fat and Dachsous and the regulation of planar cell polarity in the Drosophila wing. *Development* **131**, 3785-3794.
Mellman, I. and Nelson, W. J. (2008). Coordinated protein sorting, targeting and distribution in polarized cells. *Nat. Rev. Mol. Cell. Biol.* **11**, 833-845.
Mir, A. and Heasman, J. (2008). How the mother can help: studying maternal Wnt signaling by anti-sense-mediated depletion of maternal mRNAs and the host transfer technique. *Methods Mol. Biol.* **469**, 417-429.
Morgan, R., El-Kadi, A. M. and Theokli, C. (2003). Flamingo, a cadherin-type receptor involved in the Drosophila planar polarity pathway, can block signaling via the canonical wnt pathway in Xenopus laevis. *Int. J. Dev. Biol.* **47**, 245-252.
Nakaya, M., Fukui, A., Izumi, Y., Akimoto, K., Asashima, M. and Ohno, S. (2000). Meiotic maturation induces animal-vegetal asymmetric distribution of aPKC and ASIP/PAR-3 in Xenopus oocytes. *Development* **127**, 5021-5031.
Neuman-Silberberg, F. S. and Schupbach, T. (1993). The Drosophila dorsoventral patterning gene gurken produces a dorsally localized RNA and encodes a TGF alpha-like protein. *Cell* **75**, 165-174.
Nilson, L. A. and Schupbach, T. (1999). EGF receptor signaling in Drosophila oogenesis. *Curr. Top. Dev. Biol.* **44**, 203-243.

Roberts, S. J., Leaf, D. S., Moore, H. P. and Gerhart, J. C. (1992). The establishment of polarized membrane traffic in Xenopus laevis embryos. *J. Cell Biol.* **118**, 1359-1369.
Simon, M. A. (2004). Planar cell polarity in the Drosophila eye is directed by graded Four-jointed and Dachsous expression. *Development* **131**, 6175-6184.
Strutt, D. I. (2001). Asymmetric localization of frizzled and the establishment of cell polarity in the Drosophila wing. *Mol. Cell* **7**, 367-375.
Strutt, H. and Strutt, D. (2002). Planar polarity: photoreceptors on a high fat diet. *Curr. Biol.* **12**, R384-R385.
Tao, H., Suzuki, M., Kiyonari, H., Abe, T., Sasaoka, T. and Ueno, N. (2009). Mouse prickle1, the homolog of a PCP gene, is essential for epiblast apical-basal polarity. *Proc. Natl. Acad. Sci. USA* **106**, 14426-14431.
Taylor, J., Abramova, N., Charlton, J. and Adler, P. N. (1998). Van Gogh: a new Drosophila tissue polarity gene. *Genetics* **150**, 199-210.
Tian, A. G. and Deng, W. M. (2008). Lgl and its phosphorylation by aPKC regulate oocyte polarity formation in Drosophila. *Development* **135**, 463-471.
Tree, D. R., Shulman, J. M., Rousset, R., Scott, M. P., Gubb, D. and Axelrod, J. D. (2002). Prickle mediates feedback amplification to generate asymmetric planar cell polarity signaling. *Cell* **109**, 371-381.
Usui, T., Shima, Y., Shimada, Y., Hirano, S., Burgess, R. W., Schwarz, T. L., Takeichi, M. and Uemura, T. (1999). Flamingo, a seven-pass transmembrane cadherin, regulates planar cell polarity under the control of Frizzled. *Cell* **98**, 585-595.
van Eeden, F. and St Johnston, D. (1999). The polarisation of the anterior-posterior and dorsal-ventral axes during Drosophila oogenesis. *Curr. Opin. Genet. Dev.* **9**, 396-404.
Vinson, C. R., Conover, S. and Adler, P. N. (1989). A Drosophila tissue polarity locus encodes a protein containing seven potential transmembrane domains. *Nature* **338**, 263-264.
Vladar, E. K., Antic, D. and Axelrod, J. D. (2009). Planar cell polarity signaling: the developing cell's compass. *Cold Spring Harb. Perspect. Biol.* **1**, a002964.
Wansleeben, C. and Meijlink, F. (2011). The planar cell polarity pathway in vertebrate development. *Dev. Dyn.* **240**, 616-626.
Wolff, T. and Rubin, G. M. (1998). Strabismus, a novel gene that regulates tissue polarity and cell fate decisions in Drosophila. *Development* **125**, 1149-1159.
Yang, C. H., Axelrod, J. D. and Simon, M. A. (2002). Regulation of Frizzled by fat-like cadherins during planar polarity signaling in the Drosophila compound eye. *Cell* **108**, 675-688.
Yisraeli, J. K., Sokol, S. and Melton, D. A. (1990). A two-step model for the localization of maternal mRNA in Xenopus oocytes: involvement of microtubules and microfilaments in the translocation and anchoring of Vg1 mRNA. *Development* **108**, 289-298.
Zeng, H., Hoover, A. N. and Liu, A. (2010). PCP effector gene Inturned is an important regulator of cilia formation and embryonic development in mammals. *Dev. Biol.* **339**, 418-428.